

Equilibrium rotation in field-reversed configurations

Loren Steinhauer

Redmond Plasma Physics Laboratory, University of Washington,
4700 N. E. 95th Street, Suite 100, Redmond, Washington 98052, USA

(Received 25 October 2007; accepted 12 December 2007; published online 29 January 2008)

The turbulence that drives anomalous transport in field-reversed configurations (FRCs) is believed to break the otherwise closed magnetic surfaces inside the separatrix. This places electrons in the core of the plasma in electrical contact with those in the periphery. This effect was proposed and investigated in the context of spheromaks [D. D. Ryutov, *Phys. Plasmas* **14**, 022506 (2007)]. The opening up of internal magnetic field lines serves to regulate the electrostatic potential in the interior of the plasma, and in turn drives ion rotation. In effect, “end-shortening,” a well-known phenomenon in the FRC scrape-off layer, also extends into the plasma interior. For conditions relevant to experiments, the ion rotation can be expressed in terms of equilibrium properties (density and temperature gradients) and as such is the “equilibrium” rotation. This theory is incomplete in that it neglects evolving, transport-related effects that modify the equilibrium and, indirectly, the rotation rate. Consequently, the equilibrium rotation theory is only partially successful in predicting experimental results: although it predicts the average rotation well, the estimated degree of rotational shear seems unlikely, especially at late times in the plasma lifetime. © 2008 American Institute of Physics. [DOI: 10.1063/1.2834271]

I. INTRODUCTION

A mechanism for ion rotation in field-reversed configurations (FRCs) is introduced that is based on equilibrium properties. It follows the breaking of magnetic surfaces (by plasma turbulence) and the consequent opening of magnetic field lines. This mechanism was recently investigated by Ryutov in the context of spheromaks.¹ The same effect is expected to appear in FRCs.

Since several mechanisms for FRC rotation have already been proposed, a key question at the outset is, how does this new theory differ from the others? First, note that the new theory addresses the rotation in the interior of the plasma, i.e., inside the separatrix. The rotation of the peripheral plasma layer (scrape-off layer) is well known to result from end-shortening effects, which drive shear-Alfvén waves that quickly “spin-up” this layer.² The issue, however, is what causes the interior of the plasma, which supposedly is not exposed to end-shortening effect, to spin up. The common picture presumes the following sequence: (i) transport processes (e.g., viscosity,² particle-loss,³ or flux loss⁴) exert a mechanical torque on the ions in the interior of the plasma; (ii) as a result, the ions begin to rotate; and (iii) the electrostatic potential ϕ simply “floats” in response to the ion rotation. Expressed as cause-effect, a transport mechanism causes ion rotation that, in turn, sets up the electrical potential. By contrast, the new “equilibrium” theory proposes a quite different sequence. (i) The ambient turbulence breaks magnetic surfaces, opening up magnetic field line pathways between the core and periphery of the plasma. (ii) The highly mobile electrons quickly establish electrical contact along the opened lines, setting up a quasisteady electrical potential set by equilibrium gradients. (iii) The potential then, in combination with the diamagnetic drift, determines the ion rotation. In terms of cause-effect, the sequence is reversed from

the previous theories: the ion rotation is the *result* rather than the cause of the electrical potential.

The difference between these perspectives can be pictured using a motor-generator analogy. The older theories are analogous to a generator: the armature is turned by some mechanical force; in the presence of a magnetic field, the rotating armature creates an electrical potential that can drive a current. In short, mechanical torque creates electricity. The new equilibrium theory of rotation is analogous to a motor: a transient electrical current rapidly sets up a quasistatic (equilibrium) electrical potential in the plasma interior; this, in turn, drives plasma rotation. In short, electricity drives rotation.

The older and new principles also differ in terms of the equilibrium, *per se*. In the older theories, the interior of the plasma is “free-wheeling,” i.e., the ion rotation profile $\Omega(\psi)$ is an arbitrary function in the same way as $p(\psi)$ and $I(\psi)$. These arbitrary functions are determined by factors independent of the equilibrium, namely transport processes. In the new theory, however, the plasma rotation is *not* free but depends on properties of the equilibrium. The linchpin is the electrical contact between the plasma core and periphery. This occurs almost instantly because of the high mobility of electrons along the “opened” field lines. As such, this “electrical” mechanism should set in much more rapidly and with greater vigor than the relatively slow transport-related mechanisms. Even so, the new equilibrium theory of rotation is incomplete in that it neglects the eventual effect of the slower, transport-related processes.

The importance of ion rotation in FRCs has been well known from the earliest experiments because of a deleterious result: it drives a rotational instability that rapidly disrupts the plasma. Indeed, the rotational mode has been the dominant instability from the beginning of FRC research. It most

commonly appears as a mode with azimuthal mode number $n=2$. The review paper by Tuszewski shows experimental examples for rotational instability as well as giving references from a number of experiments.⁵ Despite the ubiquity of this mode, investigation of FRC rotation more or less ceased in the early 1980s for two reasons: (i) the discovery that applied multipoles can suppress the rotational mode, and (ii) the emergence of theories predicting that the faster-growing “tilt mode” is more dangerous in larger FRCs. The fact that *disruptive* tilting in elongated FRCs has not been confirmed has not unseated it as the chief specter threatening the progression of FRCs toward fusion energy applications. Thus, rotational instability persists as the dominant instability *in experiments*. It is important, therefore, to revisit the question of FRC rotation and to entertain new ideas both for understanding as well as possibly controlling or exploiting plasma rotation.

The outline of the paper is as follows. Section II examines the “connection length” between the core and periphery of the plasma and the time scale for electrons to approach equilibrium along opened field lines. It is shown that in typical FRCs, this equilibrium is established on a time scale much shorter than the plasma lifetime, i.e., the electrons are in mechanical equilibrium along the opened field lines. This gives rise to an easily determined electrical potential structure throughout the plasma. Section III derives the resulting ion rotation. Section IV applies this predicted rotation rate to a compendium of FRC experimental examples. This is compared to experimental observations of average rotation rate, rotational instability, and expectations about rotational shear. The paper concludes in Sec. V with a summary and discussion.

II. BROKEN-SURFACE POTENTIAL IN FRCs

A. Mechanical equilibrium of electrons along field lines

The parallel (to the magnetic field) component of the electron equation of motion is

$$m_e n \left(\frac{du_e}{dt} \right)_{\parallel} = - \frac{\partial p_e}{\partial s} + en \frac{\partial \phi}{\partial s} - 0.71 nk \frac{\partial T_e}{\partial s}, \quad (1)$$

where s is the coordinate along an opened magnetic field line, $p_e = nkT_e$ is the electron pressure (assuming a charge state $Z=1$), and m_e , n and T_e are the electron mass, density, and temperature, respectively. The last term is the parallel thermal force. Inspection of Eq. (1) suggests that $\tau_{e\parallel}$, the time scale for electrons to establish equilibrium along a field line, is given by $m_e n v_{te} / \tau_{e\parallel} \sim nkT_e / L_c$, where $v_{te} = (kT_e / m_e)^{1/2}$ is the electron thermal speed and L_c is the connection length between the core and periphery of the plasma along the opened field line. Then the *electron inertial time* to establish equilibrium is

$$\tau_{e\parallel} = L_c / v_{te}. \quad (2)$$

The inertial time $\tau_{e\parallel}$ is proportional to the connection length along an opened field line from the plasma core to periphery. In relatively quiescent plasmas, the connection path along “opened” field lines makes many circuits around the mag-

netic axis and/or the geometric axis. Thus the *connection length* L_c is much longer than the minor radius of the plasma. Among the various toroidal confinement systems, an FRC should have the shortest connection lengths because its toroidal magnetic field is small. Indeed, L_c in an FRC should be shorter than an equivalent plasma with a nominal safety factor q by a ratio of $\sim (1+q^2)^{1/2}$.

In the limit $\tau_{e\parallel} \ll \tau_N$ (particle confinement time), the electrons quickly establish an equilibrium so that the inertial term in the equation of motion can be ignored. This is equivalent to the “mechanical equilibrium” limit identified by Ryutov¹ and verified in the context of spheromaks. If this limit applies, then the inertial term in Eq. (1) can be ignored, and the force terms on the right side of the equation are in balance. It is shown next that this limit applies in typical FRC experiments.

Estimate the connection length as follows. The radial amplitude of the field line excursion is $\delta r = \delta B_{\perp} / B_0 k_{\parallel}$, where $\delta B_{\perp} / B_0$ is the relative amplitude of the transverse field fluctuation and k_{\parallel} is the *parallel* (to the ambient field B_0) wave number of the turbulence. The most unstable turbulence should have the lowest k_{\parallel} that fits onto the elongated magnetic surfaces, i.e., $k_{\parallel} = \pi / l_{\parallel}$, where l_{\parallel} is the axial length of the roughly straight section of an elongated surface. Then the radial excursion associated with a single circuit around the magnetic axis is $\delta r = (\delta B_{\perp} / B_0) l_{\parallel} / \pi$. The connection length L_c is defined as the distance along a single poloidal circuit of the magnetic axis, $2l_{\parallel}$, multiplied by the number of “steps” between the magnetic axis and the separatrix, $N = r_s / 2 \delta r$, where $r_s / 2$ is the average “minor radius” (r_s is the separatrix radius at the midplane), giving $L_c = \pi r_s (B_0 / \delta B_{\perp})$. This resembles Ryutov’s estimate [Eq. (6) of Ref. 6], although this estimate is larger by a factor of 2π . It remains to estimate the amplitude of the magnetic fluctuation. Following Krall,⁷ the saturated fluctuation for electromagnetic turbulence is $\delta B_{\perp} / B_0 = \varepsilon \rho_i / L_n$, where ρ_i is the ion gyroradius and $L_n \equiv -n (dn/dr)^{-1}$ is the local density gradient scale length. Krall estimated the proportionality factor to be in the range $\varepsilon \sim 1/5 - 1/10$. Combining these gives the connection length

$$L_c = \pi L_n r_s / \varepsilon \rho_i. \quad (3)$$

Since both L_n and ρ_i vary greatly over the cross section, an average is needed that accounts for the spatial variations. In Appendix A, this is found to be

$$L_c \approx 0.78 r_s r_c / \rho_{i0}, \quad (4)$$

where r_c is the magnetic coil radius and ρ_{i0} is the ion gyroradius based on the external magnetic field. The appearance r_c reflects the application of the axial force balance condition. With this one can find the inertial time $\tau_{e\parallel}$, Eq. (2), to establish electron equilibrium along a field line.

A comparison between typical values of $\tau_{e\parallel}$ and the plasma lifetime can be found by reference to the FRC data compendium described in Appendix B. This is a collection of results from 51 representative experimental conditions drawn from several θ -pinch-based FRC facilities. Figure 1 compares $\tau_{e\parallel}$ and τ_N (particle confinement time). The inertial time is typically $\tau_{e\parallel} \sim \tau_N / 300$ for most of the data set, the exception being the smaller (“Japan”) and translation-formation

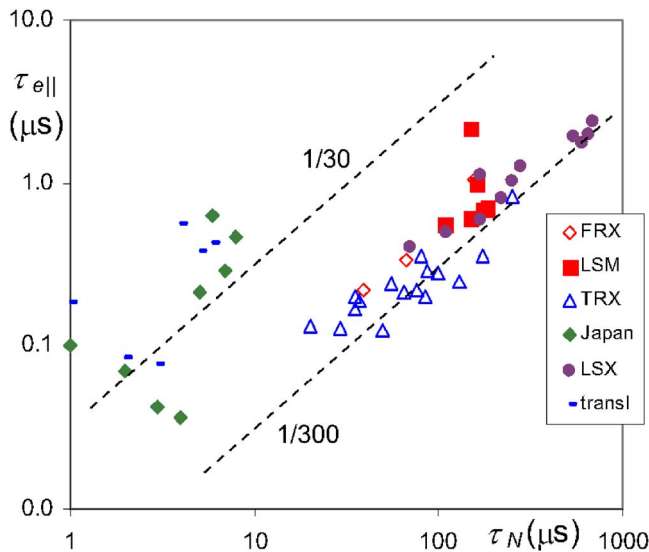


FIG. 1. (Color online) Comparison of electron inertial time and particle confinement time for FRC data set.

(“trans”) examples, for which $\tau_{e||} \sim \tau_N/30$. Therefore, the mechanical equilibrium limit applies, in which the forces [terms on the right side of Eq. (1)] are in balance.

The mechanical equilibrium of electrons along field lines in the scrape-off layer (SOL) of FRCs is well known, and has been called “end shorting.”^{2,8} The novelty here is that the electrical contact applies not only in the SOL, but extends into the plasma interior as well. This gives rise to the “broken-surface potential,” which is found next.

A consequence of opening up the field lines in the interior is the possibility of greatly enhanced electron thermal loss. This effect is not as dangerous as it might seem because of ambipolar effects: charge neutrality insures that electrons cannot be lost faster than the ions. Indeed, it has been shown that in the SOL, which directly connects to the cold material walls, the electron thermal loss is convective. The energy lost is only several kT_e per ion-electron pair escaping.⁹ This transport rate is much lower than thermal conduction for the simple reason that the mean free path is too long for the thermal conduction expression to be valid. The same should apply in the plasma interior.

B. Electrostatic potential

For the mechanical equilibrium limit, the inertial term (left side) of Eq. (1) can be ignored. This leaves a simple differential equation for the electrostatic potential,

$$\frac{\partial \phi}{\partial s} = \frac{k}{e} \left(T_e \frac{\partial}{\partial s} \ln n + 1.71 \frac{\partial T_e}{\partial s} \right). \quad (5)$$

Since the field lines wander between the core and periphery, the foregoing equation can be generalized to a *globally valid* relation governing the toroidally averaged values $\langle \phi \rangle$, $\langle n \rangle$, $\langle T_e \rangle$, and $\partial/\partial s \rightarrow \nabla$. (Hereafter, toroidally averaged values will be assumed and the $\langle \dots \rangle$ notation dropped.) Once this is recognized, the potential in Eq. (5) becomes the *broken-surface potential*.

Similar to Ref. 1, suppose the temperature and density are related by an equation of state $T_e \propto n^{\eta_e}$ (barotropic equation) where $\eta_e = \text{const}$ is the familiar parameter for the ratio of temperature-to-density gradients. With this Eq. (5) integrates at once, giving the broken surface potential

$$\phi = (1/\eta_e + 1.71)kT_e/e + \text{const}. \quad (6)$$

For a perfectly flat temperature profile ($\eta_e = 0$), the first term in Eq. (6) is replaced by $(kT_e/e) \ln n$.

III. “EQUILIBRIUM” ION ROTATION

Electron physics on opened field lines determines the electrostatic potential structure in the interior of the plasma. The resulting radial electric field, in combination with the diamagnetic drift effect, determines the ion rotation. In this section, the resulting “equilibrium” ion rotation rate is found using a simple analytic model. The descriptor “equilibrium” indicates the neglect of friction forces associated with transport (e.g., resistivity, viscosity) as well as transient effects (the inertia of ion spin-up).

To facilitate an analytic solution, adopt certain simplifications. For the physics, neglect the gyroviscous correction to the radial force balance, and assume a barotropic equation of state for the ions ($T_i \propto n^{\eta_i}$), where, for simplicity, $\eta_i = \eta_e = \eta$ is assumed. For the equilibrium, a simplified structure is adopted: the FRC is highly elongated, the toroidal field is negligible, and the ion flow is purely rotational. With high elongation, all variables depend only on r (cylindrical coordinates r, θ, z are employed). Then the radial component of the ion equation of motion reduces to a mechanical force balance,

$$0 = -\frac{1}{n} \frac{dp_i}{dr} + e \left(-\frac{d\phi}{dr} + u_{\theta} B_z \right), \quad (7)$$

where $p_i = nkT_i$ is the ion pressure. Substituting the broken-surface potential Eq. (6) and the equations of state $T \propto n^{\eta}$, the ion rotation frequency $\Omega_i \equiv u_{i\theta}/r$ becomes

$$\Omega_i = \left(1 + \eta + (1 + 1.71\eta) \frac{T_e}{T_i} \right) \frac{kT_i}{eB} \frac{1}{nr} \frac{dn}{dr}. \quad (8)$$

Thus the rotation with the broken surface potential depends on the local gradients of the density and temperature (through η).

IV. APPLICATION TO FRC EXPERIMENTS

A. Inferring experimental structure

The goal of this section is to extract the predicted rotation rate Eq. (8) for FRC experiments. One complication is that $\Omega(r)$ depends on the radial profiles of the density, temperatures, and magnetic field. No complete set of measurements of $n(r)$, $T_e(r)$, and $B_z(r)$ are available for *any* experiments. Despite this difficulty, certain factors act in our favor. The radial pressure balance that applies in elongated FRCs as well as the axial-force balance (“average- β ”) condition allow one to infer the gross internal structure from a much more limited set of measurements. A practical approach assumes that the profiles belong to a flexible, multiparameter family

of functions. Then basic measurements from experiments—the separatrix radius r_s , the average density, the total temperature $T_e + T_i$ (inferred from pressure balance), and the external magnetic field B_e —can be used to pin down the parameters. This yields plausible profiles for n , T_i , T_e , and B_z . The specific method applied here is the “two-point equilibrium” (2PE) model introduced in Appendix C. This model is applied to the FRC data compendium that was described in Appendix B.

For convenience, express the rotation frequency in terms of the minor radius variable $u \equiv 2r^2/r_s^2 - 1$, where $u=0$ is the magnetic axis and $u=1$ is the separatrix. Then the equilibrium rotation frequency is

$$\Omega_i(u) = \left(1 + \frac{1 + 1.71\eta T_e}{1 + \eta T_i}\right) \Omega_0 \frac{n_m db}{n du} \quad \Omega_0 \equiv -\frac{8kT_{i,m}}{eB_e r_s^2}, \quad (9)$$

where $T_{i,m}$, n_m are the maximum ion temperature and density and B_e is the external field. Here $b(u)$ and $n(u)/n_m$ are field and density profiles inferred using the 2PE model (Appendix C).

B. Average rotation rate

Compare the predicted rotation frequency with experiment. While Eq. (9) gives the Ω_i profile, typical experimental measurements yield only a single “averaged” rotation frequency (with only one or two exceptions). The density weighted an average value of Ω_i is

$$\bar{\Omega}_i \equiv \frac{1}{N} \int_{-1}^1 \Omega \frac{n}{n_m} du, \quad N \equiv \int_{-1}^1 \frac{n}{n_m} du. \quad (10)$$

With Eq. (9), the numerator in the left-hand side of Eq. (10) can be integrated analytically. Then

$$\bar{\Omega}_i \equiv \left(1 + \frac{1 + 1.71\eta T_e}{1 + \eta T_i}\right) \Omega_0 \frac{2b_1}{N}. \quad (11)$$

Here the temperature ratio T_e/T_i is assumed to be uniform. The customary *yardstick* for the rotation rate is the ion diamagnetic drift frequency, which in elongated FRCs is $\Omega_* = (1/ernB_z) dp_i/dr$. In general, Ω_* varies with radius, although it is uniform in a rigid-rotor profile, for which $B_z = B_e \tanh Ku$, $n = n_m \operatorname{sech}^2 Ku$, and $T_i = \text{const}$. The axial force balance condition (re Appendix A) fixes the shape parameter $K \approx (3/2)^{1/2} r_s/r_c$ (an approximation is based on the small- K expansion.) Then for a rigid rotor

$$(\Omega_*)_{RR} \approx (3/2)^{1/2} (r_s/r_c) \Omega_0. \quad (12)$$

The $\bar{\Omega}_i$ predicted by equilibrium rotation theory Eq. (11) and $(\Omega_*)_{RR}$ are calculated using parameters from the FRC data compendium (Appendix B): the results are shown in Fig. 2. The bulk of the examples falls in the range $\bar{\alpha} \equiv \bar{\Omega}_i/(\Omega_*)_{RR} = 2-2.5$. Compare this prediction with experiment. Most measurements of rotation date to the early 1980s when concern ran high about rotational instability. These were summarized in the 1985 review by Tuszewski.⁵ The most reliable available technique indicated a *threshold* value for the appearance of the $n=2$ rotational instability at $\Omega/\Omega_* = 1-1.2$. This compares with the theoretical predictions of marginal

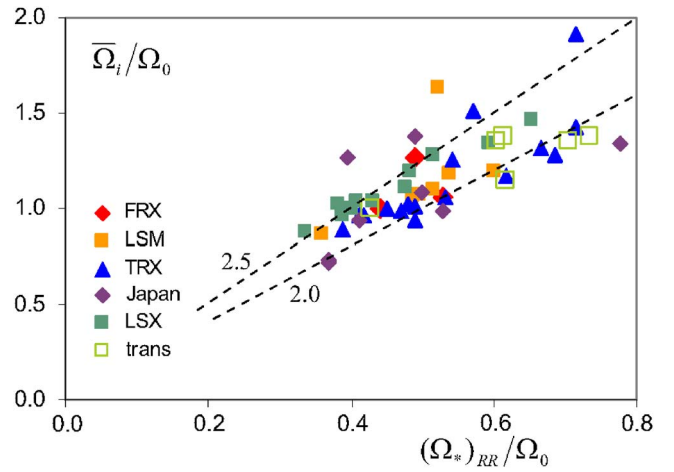


FIG. 2. (Color online) Predicted average rotation rate vs diamagnetic drift frequency for “rigid-rotor;” Ω_0 is defined in Eq. (9).

stability at $\Omega/\Omega_* = 1.2-1.4$ (finite-Larmor radius theory) and $1.3-1.5$ (Vlasov theory).⁵ The prediction in Fig. 2 of $\Omega/\Omega_* \sim 2-2.5$ is consistent with the nearly ubiquitous appearance of the rotational instability in experiments in that this rotation rate is above the instability threshold. Notable exceptions to this “rule” are FRCs formed by ejection-translation (marked “trans” in Fig. 2), which generally exhibited no instability. This may be because these examples have a small toroidal field, which apparently has a significant stabilizing effect.⁶

C. Velocity shear and stabilization

The predicted equilibrium rotation profile $\Omega(u)$, Eq. (9), varies from experiment to experiment. Figure 3 shows the profile for two examples adapted using the 2PE model: a medium-size FRC from TRX-2 with flux and particle confinement times of $\tau_\phi = 85 \mu\text{s}$ and $\tau_N = 80 \mu\text{s}$, and a large FRC from LSX with $\tau_\phi = 475 \mu\text{s}$ and $\tau_N = 550 \mu\text{s}$. The horizontal black lines are the average values $\bar{\Omega}_i/2\pi$ (90 and 19 kHz,

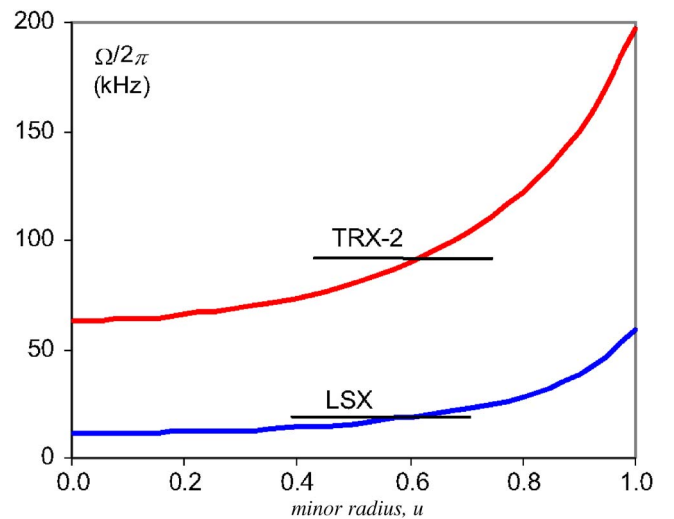


FIG. 3. (Color online) Rotation frequency profile for examples from TRX-2 and LSX.

TABLE I. Stability prediction for examples.

	r_s/r_c	$x_{s,cr}$
TRX-2	0.47	0.62
LSX	0.48	1.21

respectively). Both examples in Fig. 3 exhibit strongly sheared flows with rotation frequency a factor of 3 (TRX-2) and 5 (LSX) times higher at the separatrix than the magnetic axis.

A crude criterion for flow-shear stabilization is $V' > \gamma$, where γ is the growth rate for the instability in question and V' is the flow shear. While more sophisticated forms of this have been developed elsewhere (see, e.g., Ref. 21), the crude criterion is adopted here as a rule of thumb. For pure rotation, the flow shear is $V' = r d\Omega_i/dr$. Consider a rough average of the flow shear based on the region between the magnetic axis and separatrix, which is the region where the gravitational effect is destabilizing,

$$V' \approx |\Omega_i(1) - \Omega_i(0)|\bar{r}/\Delta r. \quad (13)$$

Use for the mean radius $\bar{r} \rightarrow R$ and the minor radius $\Delta r \rightarrow r_s/2 = R/\sqrt{2}$. Then with Eq. (9),

$$V' \approx (1 \dots) \Omega_0 \left[\left(\frac{n_m}{n} \frac{db}{du} \right)_1 - \left(\frac{n_m}{n} \frac{db}{du} \right)_0 \right]. \quad (14)$$

The factor (1...) [Eq. (11)] slightly exceeds unity for expected conditions, e.g., for $\eta \sim 0.25$, $T_e/T_i \sim 0.5$, (1...) = 1.1, which is assumed as a typical value in what follows. The growth rate for the $n=2$ rotational mode is $\gamma \approx \Omega$ in a θ pinch plasma.⁵ In FRCs, the growth rate is comparable so $\gamma \approx \Omega$ is assumed. Then with a typical average rotation rate $\bar{\Omega}_i \approx 1.6\Omega_{*RR}$ (Fig. 2), the growth rate is

$$\gamma \approx 2(r_s/r_c)\Omega_0. \quad (15)$$

Substitute Eqs. (14) and (15) into the crude stability criterion, $\gamma < |\nabla u|$: then stability requires

$$r_s/r_c < x_{s,cr} \equiv 0.55(\dots), \quad (16)$$

where the factor (...) is the same as that in Eq. (14). Table I compares the radius ratio r_s/r_c to the predicted maximum value for stability. Both examples easily satisfy the crude stability criterion, with LSX by a wide margin. This agrees with the usual observation of stability at early times, but conflicts markedly with the regular appearance of the rotational instability at “late times,” i.e., after a stable period comparable to τ_N . The origin of the latter disagreement is discussed in the next section.

V. DISCUSSION

The opening of magnetic surfaces by plasma turbulence sets up a particular electrostatic potential throughout the FRC and, from that, the ion rotation rate. This rate depends on quantities associated with the equilibrium, *per se*: as such it is called “equilibrium rotation.” The predicted *average* rotation rate is consistent with observations in that it is above

the threshold for the rotational instability, which is almost always observed. On the other hand, equilibrium rotation theory predicts considerable flow shear. Using a simple flow-shear stability criterion, the predicted flow shear is more than adequate to guarantee stability. This is consistent with the early stable behavior in FRCs but fails to predict the nearly ubiquitous late-time appearance of rotational instability.

The common interpretation of the late-time arrival of the rotational instability is as follows. Finite ion gyroradius effects, which are stabilizing, give rise to a stability threshold in the range $\Omega/\Omega_* = 1.2-1.5$, assuming rigid rotation of the ions. It is supposed that the FRC starts out with a small rotation rate (nominally zero), well below the threshold. However, over the lifetime of the plasma, the rotation rate gradually rises due to frictional effects (e.g., viscosity). Eventually it exceeds the threshold and instability sets in. This scenario would explain the late-time arrival of the rotational instability.

However, an alternate explanation takes into account the “equilibrium rotation” concept developed here. Rotation sets in very quickly but is quite concentrated near the edge. This state is stabilized by flow shear. However, over the lifetime of the plasma, frictional effects gradually modify the gradients and flatten the $\Omega(r)$ profile. Eventually the flow shear falls below the threshold, i.e., V' no longer exceeds γ , unleashing the rotational instability.

A proper exploration of these two possibilities requires a model incorporating both the radial (r) and azimuthal (θ) components of the ion equation of motion. The r equation gives the ion rotation in terms of the radial electric field and the diamagnetic drift. Both of these, however, depend on the “equilibrium” density and temperature gradients, which slowly evolve according to the θ equation. Prominent in the θ equation are the rotational inertia (giving rise to transient effects) and friction forces (resistive and viscous). The viscous force arises from shear in the “equilibrium” rotation given by the r equation. Thus the r and θ equations are intimately coupled. Neglect of this coupling leads to the present dilemma. The equilibrium rotation theory, as developed here, considers the r component in isolation, assuming that the gradients are merely a given feature of the equilibrium. Previous models consider the θ component in isolation. A comprehensive model will account for both and their intercoupling.

APPENDIX A: AVERAGED CONNECTION LENGTH

An averaged value of the connection length comes from converting Eq. (3) into a differential relation,

$$dL_c/dr = \pi L_n/\varepsilon \rho_i, \quad (A1)$$

where L_n and ρ_i are local values. Assume a rigid rotor profile: $B = B_e \tanh(Ku)$ and $n = n_m \operatorname{sech}^2(Ku)$, where B_e is the external magnetic field, n_m is the maximum density, $u \equiv 2r^2/r_s^2 - 1$ is the “minor radius” variable, and K is the profile shape parameter. Integrate Eq. (A1) on the range $r = r_s/\sqrt{2}$ to r_s ,

$$L_c = \frac{\pi \ln 2}{16\epsilon K} \frac{r_s^2}{\rho_{i0}}. \quad (\text{A2})$$

Introduce the axial force balance relation (average- β condition) for a constant-radius flux conserver at $r=r_c$: $\langle\beta\rangle = \tanh K/K = 1 - r_s^2/2r_c^2$, and employ the small- K expansion so that $K \approx (3/2)^{1/2} r_s/r_c$. Then

$$L_c = \frac{\pi \ln 2}{16(3/2)^{1/2}\epsilon} \frac{r_s r_c}{\rho_{i0}}. \quad (\text{A3})$$

Finally, with an intermediate value of $\epsilon=1/7$, this gives $L_c = 0.78 r_s r_c / \rho_{i0}$.

APPENDIX B: UPDATED FRC DATA COMPENDIUM

A compendium of FRC equilibrium and confinement data was collected and published several years ago.¹¹ These examples were for long-lived, quiescent, stable FRCs formed by the θ -pinch method. The original collection has been augmented to include several examples representing other experiments: “Translation-Confinement-Sustainment” (TCS),^{10,12} “STP,”¹³ and “FRC Injection Experiment” (FIX).¹⁴

Direct measurements of the electron temperature were taken in a relatively small fraction of the examples in the compendium. Thus, when needed, the electron temperature is estimated using the formula

$$T_e = T_i \{3 - \exp[-(T_i/250)^4]\}, \quad (\text{B1})$$

where $T_t = T_i + T_e$ is the total temperature inferred using “pressure balance,” and the units are eV. This expression was chosen so that T_e/T_t has the asymptotic value 1/3 for large T_t and $T_e \rightarrow T_t/2$ for low temperature. The former corresponds roughly to high-temperature experiments where both T_e and $T_i + T_e$ were measured; the latter springs from the expectation that at low temperature, electron-ion equilibration will be so fast that the two temperatures will be approximately equal.

APPENDIX C: TWO-POINT EQUILIBRIUM MODEL

Suppose the magnetic field structure is given by the family of functions $B_z = B_e b(u; \dots)$, where B_e is the external field and $b(\dots)$ is a suitable function of the minor radius variable $u = 2r^2/r_s^2 - 1$ and a set of adjustable parameters. Pressure balance gives the total pressure p_t (ion+electron) $p_t = (B_e^2/2\mu_0) \times (1 - b^2)$. The total temperature (ion+electron) follows at once from this and the barotropic relations $T_t = T_{t,m}(1 - b^2)^{\eta/(1+\eta)}$. Distinct ion and electron temperatures can be extracted as described in Appendix B.

This system contains several global parameters. Routinely inferred in FRC experiments are r_s , B_e , and $T_{t,m}$ (by pressure balance with the average density from interferometry). This leaves only the adjustable parameters in $b(u; \dots)$ to determine. Adopt the following family of functions:

$$b(u; b_1, \sigma) = b_1 u e^{\sigma(u^2-1)} \quad (\text{C1})$$

with two parameters b_1 (the normalized field at the separatrix $u=1$) and σ (to which the gradient at the separatrix will be

set). This form satisfies the requirement that the field vanish at the magnetic axis $u=0$. Two conditions are needed to fix these two parameters: (i) the axial force balance (average- β condition) and (ii) the density gradient length scale at the separatrix $L_n \equiv [-n(dn/dr)^{-1}]_{r_s}$ is prespecified.

The axial force balance condition is $\langle\beta\rangle = 1 - r_s^2/2r_c^2$, where $\beta \equiv p_t/(B_e^2/2\mu_0)$ is based on the external magnetic field and $p_t = (B_e^2/2\mu_0)(1 - b^2)$. The average is over the mid-plane cross section inside the separatrix. Applied to Eq. (C1), this gives

$$r_s^2/2r_c^2 = \int_0^1 b^2 du \approx 1/(3 + 2.666\sigma + 0.43\sigma^2) \quad (\text{C2})$$

accurate to within 1.2% in the typical range $-0.5 < \sigma < 2$. The separatrix boundary condition gives

$$\frac{r_s}{8L_n} = \frac{b_1^2(1 + 2\sigma)}{\Gamma(1 - b_1^2)}. \quad (\text{C3})$$

Using Eqs. (C2) and (C3), the parameters b_1 and σ are readily found using a Newton–Raphson procedure.

Two further quantities are needed, L_n and η . The edge density gradient length L_n [appearing in Eq. (3)] was inferred using several techniques in a small set of examples in the Field-Reversed Experiments (FRX-A,-B,-C), and Triggered Reconnection Experiments (TRX-1,-2) and collected in Ref. 15. In addition, measured values of L_n are reported for “PIACE,”¹⁶ FRC Injection Experiment (FIX),¹⁴ and Field-Reversed Experiment-Liner (FRX-L).¹⁷ From these measurements, the ratio L_n/l_i can be inferred, where $l_i = (m_e/\mu_0 e^2 n)^{1/2}$ is the ion inertial length (m_e is the electron mass, μ_0 is the permeability of free space, e is the electron charge, and n is the average density). The average value for these examples is $L_n/l_i = 1.52$. For the purpose of analyzing the experimental data, a typical value of $L_n/l_i = 3/2$ is assumed. The other quantity needed is the “barotropic” constant η . Simultaneous electron temperature and density profile measurements are only available from two experiments, FRX-B¹⁸ and FRX-C.^{19,20} Despite the significant data scatter, $\eta \sim 0.2$ can be inferred for FRX-B and $\eta \sim 0.3$ for FRX-C for the region inside the separatrix. For analyzing the experimental data, a typical value of $\eta = 1/4$ is assumed.

¹D. D. Ryutov, Phys. Plasmas **14**, 022506 (2007).

²L. C. Steinhauer, Phys. Fluids **24**, 328 (1981).

³A. Eberhagen and W. Grossmann, Z. Phys. **248**, 131 (1971); D. C. Barnes and C. E. Seyler, in *Proceedings of the U.S.-Japan Joint Symposium on Compact Toruses and Energetic Particle Injection* (Princeton University Press, Princeton, NJ, 1979), p. 110.

⁴T. Takahashi, H. Yamaura, F. P. Iizima, Y. Kondoh, T. Asai, Ts. Takahashi, Y. Matsuzawa, T. Okano, Y. Hirano, N. Mizuguchi, Y. Tomita, and S. Inagaki, Plasma and Fusion Res.: Rapid Commun. **2**, 008 (2007).

⁵M. Tuszewski, Nucl. Fusion **28**, 2033 (1985).

⁶H. Y. Guo, A. L. Hoffman, L. C. Steinhauer, and K. E. Miller, Phys. Rev. Lett. **95**, 175001 (2005).

⁷D. D. Ryutov, J. Kesner, and M. E. Mauel, Phys. Plasmas **11**, 2318 (2004).

⁸N. A. Krall, Phys. Fluids B **1**, 1811 (1989).

⁹L. C. Steinhauer, Phys. Plasmas **9**, 3851 (2002); note that in the analysis here, the parallel thermoelectric effect, i.e., the term multiplied by the “0.71” in Eq. (1), was overlooked.

¹⁰L. C. Steinhauer, Phys. Fluids B **4**, 4012 (1992).

¹¹N. Iwasawa, A. Ishida, and L. C. Steinhauer, Phys. Plasmas **7**, 931 (2000).

- ¹²H. Y. Guo, A. L. Hoffman, K. E. Miller, and L. C. Steinhauer, *Phys. Rev. Lett.* **92**, 245001 (2004).
- ¹³Y. Aso, S. Himeno, and K. Hirano, *Nucl. Fusion* **23**, 751 (1983).
- ¹⁴T. Ohtsuka, M. Okubo, S. Okada, and S. Goto, *Phys. Plasmas* **5**, 3649 (1998).
- ¹⁵L. C. Steinhauer, *Phys. Fluids* **29**, 3379 (1986).
- ¹⁶S. Okada, Y. Kiso, S. Goto, and T. Ishimura, *Phys. Fluids B* **1**, 2422 (1989).
- ¹⁷T. Intrator, S. Y. Zhang, J. H. Degnan, I. Furno, C. Grabowski, S. C. Hsu, E. L. Ruden, P. G. Sanchez, J. M. Taccetti, M. Tuszewski, W. J. Wagenaar, and G. A. Wurden, *Phys. Plasmas* **11**, 2580 (2004).
- ¹⁸W. T. Armstrong, R. K. Linford, J. Lipson, D. A. Platts, and E. G. Sherwood, *Phys. Fluids* **24**, 2068 (1981).
- ¹⁹D. J. Rej and W. T. Armstrong, *Nucl. Fusion* **24**, 177 (1984).
- ²⁰M. Tuszewski, *Plasma Phys. Controlled Fusion* **26**, 991 (1984).
- ²¹S. W. Ng and A. B. Hassam, *Phys. Plasmas* **12**, 064504 (2005).